

## Segregation of oxygen vacancy at metal-HfO<sub>2</sub> interfaces

Eunae Cho,<sup>1</sup> Bora Lee,<sup>1</sup> Choong-Ki Lee,<sup>1</sup> Seungwu Han,<sup>1,a)</sup> Sang Ho Jeon,<sup>2</sup> Bae Ho Park,<sup>2</sup> and Yong-Sung Kim<sup>3</sup>

<sup>1</sup>Department of Physics, Ewha Womans University, Seoul 120-750, Republic of Korea

<sup>2</sup>Department of Physics, Konkuk University, Seoul 143-091, Republic of Korea

<sup>3</sup>Korea Research Institute of Standards and Science, Daejeon 305-340, Republic of Korea

(Received 9 January 2008; accepted 21 May 2008; published online 13 June 2008)

We perform first-principles calculations on metal-HfO<sub>2</sub> interfaces in the presence of oxygen vacancies. Pt, Al, Ti, and Ag are considered as electrodes. It is found that oxygen vacancies are strongly attracted to the interface with binding energies of up to several eVs. In addition, the vacancy affinity of interfaces is proportional to the work function of metals, which is understood by the transition level of the vacancy and metal-Hf bonding. Interfacial segregation of vacancies significantly affects effective work functions of *p* metals. Our results are consistent with flatband shifts in *p*-type field effect transistors employing high-*k* dielectrics and metal gates. © 2008 American Institute of Physics. [DOI: 10.1063/1.2943322]

To cope with a leakage current problem in aggressively scaled microelectronic devices, SiO<sub>2</sub> used as gate insulators in the metal-oxide-semiconductor field effect transistor (MOSFET) is being replaced by other insulators with high dielectric constants (high-*k*). Among various materials explored to date, Hf-based high-*k* materials such as HfO<sub>2</sub>, HfON, HfSiO, and HfSiON are attracting most attention. However, the replacement gate oxides were found to give rise to many technical issues such as degradation of carrier mobility, thermal instability after annealing, or depletion of poly-Si gates.<sup>1</sup> It is now widely accepted that some of these can be resolved by switching the material for gate electrodes from poly-Si to pure metals.

The introduction of high-*k* materials in combination with metal gates can be marked as a most radical change ever faced by the semiconductor industry. Consequently, there exist several issues to be addressed to further improve the reliability of devices based on high-*k* dielectrics. For instance, it has been observed that the flatband voltage ( $V_{fb}$ ) shifts after postdeposition annealing (also known as  $V_{fb}$  roll offs).<sup>1-3</sup> This behavior is more pronounced for metal gates with high work functions (*p* metals) used in *p*-type MOSFETs. Among the various origins of  $V_{fb}$  shift elaborated so far, a mechanism based on electrically active oxygen vacancies has provided consistent explanations.<sup>1,4-9</sup> Although the defect formation energy ( $\Omega_f$ ) of the oxygen vacancy is relatively high in HfO<sub>2</sub>, they can be generated with ease in gate stacks through the oxidation of underlying Si substrates.<sup>4,7</sup>

In this letter, motivated by mounting evidence of the critical role of oxygen vacancies, we carry out first-principles calculations on oxygen vacancies in HfO<sub>2</sub> close to the metal-oxide interface in order to unravel energetics and electronic structures of the interface in the presence of oxygen vacancies. As a model system, we choose (1×1) unit cell of monoclinic-HfO<sub>2</sub> (001) surface interfaced with (2×√3) unit cell of various metals such as Pt, Ag, Al, and Ti with (111) or (0001) surface orientations. To match the lateral periodicity, we adjust lattice parameters of metals to those of HfO<sub>2</sub> (5.020×5.120 Å<sup>2</sup>). This reflects experimental conditions

that metal electrodes are deposited on top of HfO<sub>2</sub> films. The lattice mismatches between metals and HfO<sub>2</sub> are -10% -4%. In Ref. 10, the strain effect was examined for (1×1) Pt/HfO<sub>2</sub> interface by comparing results with √2×√2 model and it was concluded that the effect of strain on the electronic and thermodynamic properties of the interfaces is small. Since the lattice mismatches are similar for other metals, it is assumed that the results are not influenced much by the strain effects. The calculated work functions of the strained metals are 6.08 eV(Pt), 5.14 eV(Ag), 4.96 eV(Ti), and 4.21 eV(Al), and thus the dependence on the work function can be studied. The vacuum with a length of 12 Å is inserted between repeated metal-insulator slab models, as shown in Fig. 1(a). We start with stoichiometric interfaces.

For first-principles calculations, Vienna *ab initio* simulation package (VASP) is used throughout this work.<sup>11</sup> The projector-augmented-wave pseudopotentials<sup>12</sup> are employed to describe electron-ion interactions while the exchange-correlation energies of electrons are calculated within the

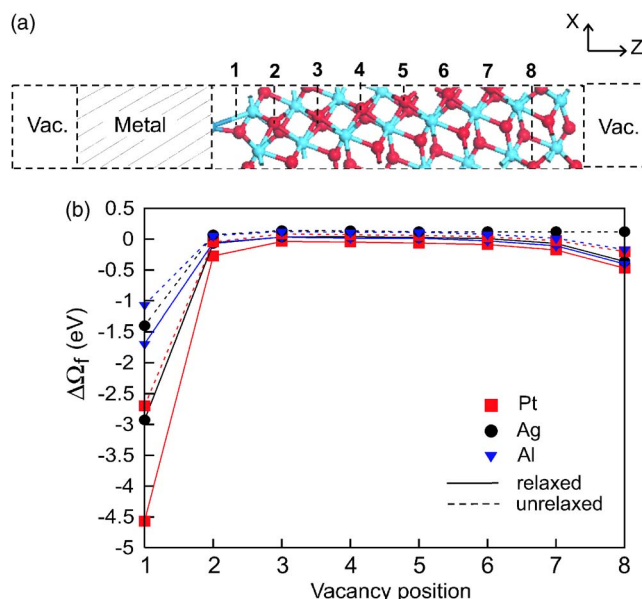


FIG. 1. (Color online) (a) Unit cell of the model interface. Vacancy positions are noted as 1–8. (b) Defect formation energies of the oxygen vacancy at the interface with respect to the bulk value ( $\Delta\Omega_f$ ).

<sup>a)</sup> Author to whom the correspondence should be addressed. Electronic mail: hansw@ewha.ac.kr.

local density approximation (LDA).<sup>13</sup> The energy cutoff for the plane-wave expansion is chosen to be 500 eV and  $k$  points are sampled on  $4 \times 4 \times 1$  meshes for Ag, Ti, and Al electrodes while  $5 \times 5 \times 1$  meshes are used for Pt. In selecting the starting interfacial structure for a specific metal electrode, the lateral unit area is divided into a  $5 \times 5$  grid with  $\sim 1$  Å spacing between grid points. The metal layers are shifted over grid points and relaxed subsequently. The structures with the lowest total energy among 25 geometries are then chosen.

Firstly, we investigate  $\Omega_f$  as an oxygen vacancy approaches the interface. The theoretical analysis in Ref. 4 shows that the density of the oxygen vacancy could be as high as  $10^{20}$ – $10^{21}$  cm<sup>-3</sup> for  $p$  metals. Assuming that the thickness of HfO<sub>2</sub> is 10 nm, the areal vacancy density is 1–10 nm<sup>-2</sup>. One vacancy per (1 × 1) unit cell corresponds to the areal density of 4 nm<sup>-2</sup>, which is within the theoretical range. The oxygen vacancy is introduced by removing a fourfold coordinated oxygen atom from one of 1–8 sites in Fig. 1(a).  $\Omega_f$  is slightly lower for the fourfold oxygen atom compared to the threefold site.<sup>14</sup> Since the vacancy state is a deep level in HfO<sub>2</sub>, we consider only the neutral charge state. Figure 1(b) shows  $\Delta\Omega_f$  ( $=\Omega_f - \Omega_{f,\text{bulk}}$ ) at the interface for three representative cases of Pt, Ag, and Al electrodes. For the sake of analysis, two types of calculations are separately presented. In “unrelaxed” calculations, atoms are frozen at their equilibrium positions determined for the vacancy-free interface. In contrast, atomic positions are optimized in “relaxed” results. For both conditions of the computation,  $\Delta\Omega_f$  remains almost constant inside the slab but drops sharply when the vacancy is right next to the metal. In particular, the reduction of  $\Delta\Omega_f$  is more pronounced for  $p$  metals (Ag and Pt) and the interfacial segregation energy of vacancies ( $E_{\text{seg}}$ ), defined as  $\Delta\Omega_f$  for the vacancy site closest to the interface, is correlated well with the work functions of metals. When ions are allowed to relax,  $E_{\text{seg}}$  is further decreased by  $\sim 2.0$  eV for Pt and Ag electrodes. These are attributed to additional Ag–Hf or Pt–Hf bonds formed at the interface region (see below).

The classical theory of interactions between oxygen vacancies and metal-oxide interfaces is based on the electrostatic interaction between ionized vacancies and induced image charges.<sup>15</sup> To estimate the charge state of the oxygen vacancy in our model systems, we examine the differential charge defined as  $\Delta\rho = \rho(\text{metal}/\text{HfO}_2) - \rho(\text{metal}) - \rho(\text{HfO}_2)$ . The inspection of  $\Delta\rho$  around the vacancy site indicates that the charge transfer is smaller than  $0.1e$ . Therefore, the image-charge interaction alone cannot fully account for the sharp drop of  $\Delta\Omega_f$  at the interface. Although the defect level of the oxygen vacancy lies above the Fermi level of Pt electrodes by  $\sim 1$  eV, a small charge transfer results in a large band bending due to the periodic repetition of vacancies in  $xy$  directions.

To examine the dependence of segregation energies on the supercell size, a calculation is performed on the Pt/HfO<sub>2</sub> interface with the length of unit cell doubled along the  $y$  direction [i.e., (1 × 2) unit cell]. The computed  $E_{\text{seg}}$  is  $-4.48$  eV which is close to  $-4.50$  eV calculated for (1 × 1) unit cell. This again indicates that  $E_{\text{seg}}$  is largely determined locally, rather than through interactions with image charges which should be sensitive to the periodicity in lateral ( $xy$ ) dimensions. We also calculate  $E_{\text{seg}}$  for the oxygen-rich inter-

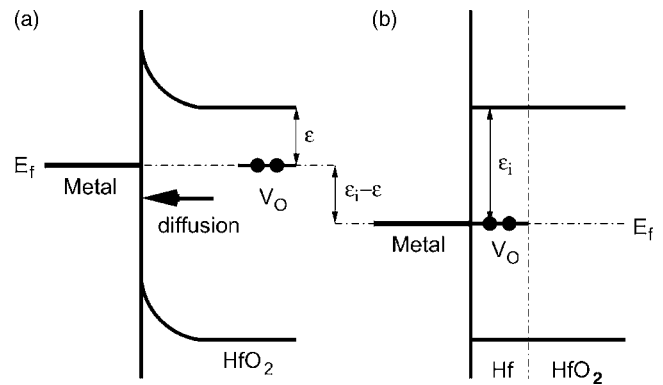


FIG. 2. Schematic band diagrams to explain the segregation energy of the oxygen vacancy ( $V_O$ ). (a) The oxygen vacancy is inside HfO<sub>2</sub>. (b) The oxygen vacancy is right at the interface.  $E_f$  is the Fermi level.

face although this type of interface is not favored against the silicon oxidation.<sup>10</sup> This is done by adding two more oxygen atoms to the interface shown in Fig. 1(a). The calculated  $E_{\text{seg}}$  is  $-4.7$  eV, again comparable to that of the stoichiometric interface.

The large  $E_{\text{seg}}$  excludes a spatial distribution of oxygen vacancies in depth, and rather implies the formation of an abrupt layer of the vacancies at the interface, notably for  $p$  metals. This result originates in part from a change of the electronic structure of the vacancy at the interface, as schematically presented in Fig. 2. When the vacancy is away from the interface, band bending such as shown in Fig. 2(a) occurs. The transition state of the oxygen vacancy in this case is mainly characterized by Hf-5d orbitals. At the interface, however, the electronic density of the defect state is mainly contributed by metallic states of the electrode. As a result, the transition level of the oxygen vacancy at the interface drops near to the Fermi level of the electrode [see Fig. 2(b)]. The transition level of the oxygen vacancy inside HfO<sub>2</sub> ( $\epsilon$ ) is about 0.9 eV below the conduction band minimum, while those at the interface ( $\epsilon_i$ ) are 1.80, 1.34, and 0.45 eV for Pt, Ag, and Al electrodes. The level drops ( $\epsilon_i - \epsilon$ ) between the oxygen vacancy in bulk and at the interface are well correlated to the unrelaxed segregation energies in Fig. 1(b). (However, underestimation of the energy gap by LDA should be taken into account for an accurate comparison.)

In order to investigate how a continuous trapping of the vacancy at metal-oxide interfaces affects the results, we remove oxygen atoms nearest to the interface successively and relax atomic structures. The results can also be used in estimating segregation effects for oxygen-deficient interfaces formed at low oxygen pressures.<sup>10</sup> A series of model interfaces of Pt/HfO<sub>2</sub> obtained in this way are displayed in Fig. 3(a). Up to three oxygen atoms are removed from the interface (V3). Beyond V1, the interfacial bonding is formed between Pt and Hf atoms and this accounts for the large energy drop between unrelaxed and relaxed  $\Delta\Omega_f$  in Fig. 1(b). In Fig. 4(a), we calculate  $E_{\text{seg}}$  for each interface. It is seen that  $E_{\text{seg}}$ 's for  $p$  metals are reduced as vacancies are accumulated at the interface and they converge to  $\sim -1$  eV. This amount of segregation energy was also observed for Si–HfO<sub>2</sub> interface,<sup>16</sup> indicating that  $E_{\text{seg}}$  in this range stems from the weakened Hf–O bonding, rather than the change in the transition level discussed in the above. In passing, we note that the entropy decreases as vacancies are entrapped at the interface, thereby increasing the free energy. Assuming that the thickness of

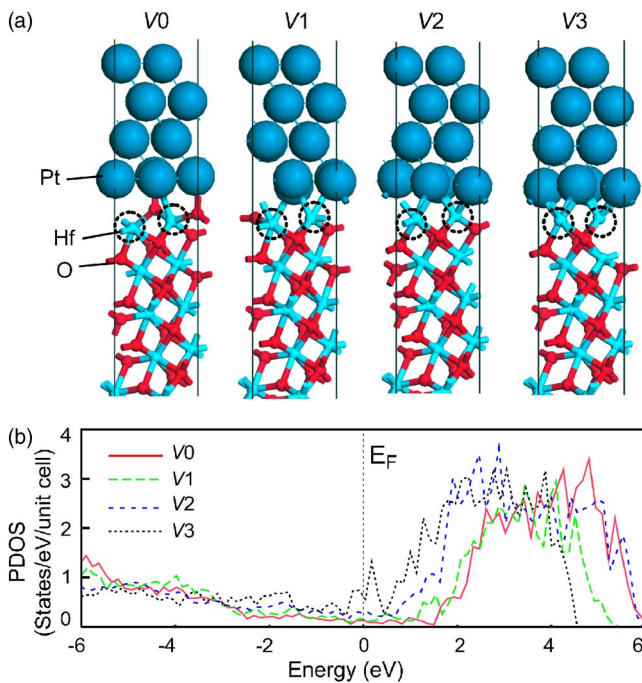


FIG. 3. (Color online) (a) The model interface with increasing number of oxygen vacancies at the interface.  $VN$  means  $N$  oxygen atoms are removed from  $(1 \times 1)$  unit cell of the stoichiometric interface. (b) The PDOS for the interfacial Hf atoms marked with dashed circles in (a). The Fermi level is set to zero.

$\text{HfO}_2$  is 5 nm, we find that the increase of free energy for the vacancy segregation is around 0.4 eV at room temperature. Therefore, the segregation for  $p$  metals is not affected much by entropic effects.

Finally, we examine the valence band offsets (VBOs) as oxygen vacancies are bound at the interface. VBOs are calculated by directly locating the Fermi level from the valence top of partial density of states (PDOS) of  $\text{HfO}_2$  layer in the middle of the slab.<sup>17</sup> As shown in Fig. 4(b), VBOs for  $p$  metals are significantly affected by the presence of the oxygen vacancy and they increase as vacancies segregate at the interface. (A dip at V1 for Pt and Ag electrodes is attributed to the formation of interfacial bonding which causes electron transfers from electrodes to Hf atom.<sup>18</sup>) In addition, VBOs for all metals tend to be pinned. This is consistent with the experimental observation that  $V_{fb}$  roll off is more serious for  $p$ -type MOSFET. Our results are also reminiscent of the

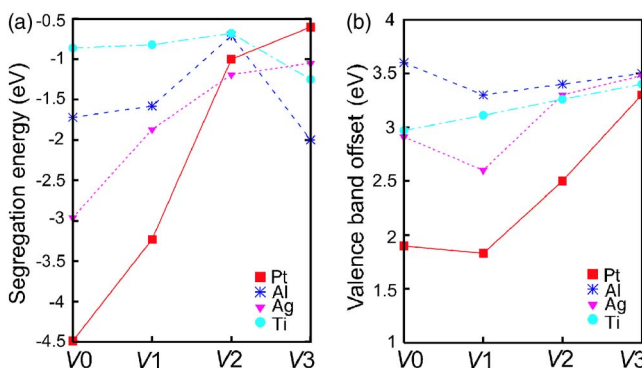


FIG. 4. (Color online) (a) The segregation energy of the oxygen vacancy as the interfacial structure changes from V0 to V3. (b) The corresponding VBOs.

vacancy-induced Fermi level pinning at Si– $\text{HfO}_2$  interface<sup>19</sup> although the microscopic origins are very different.

In order to explain the convergence of VBOs or the effective work function of metals, we plot in Fig. 3(b) PDOS for interfacial Hf atoms marked by dashed circles in Fig. 3(a). It is found that as the oxygen vacancies are accumulated at the interface, there is a substantial increase of PDOS at the Fermi level. This means that Hf atoms at the interface develop metallic characters and the Fermi level is largely determined by the metallic Hf layers rather than by the electrodes. In fact, the experimental work function of Hf metals is  $\sim 3.9$  eV which is close to the pinning point.

In summary, we found that the oxygen vacancy is strongly attracted to the interface, especially for  $p$  metals. This is due to the change in the transition levels of the oxygen vacancy and formation of interfacial bonding. The segregation of oxygen vacancy lead to substantial shifts in VBO's for the interface with  $p$  metals, due to the metallization of interfacial Hf layers. This is consistent with the  $V_{fb}$  shift observed in experiments.

This work was supported by the System IC2010 program and the National Program for 0.1 Terabit NVM Devices. E.C. was supported by the Seoul Science Fellowship. B.H.P. was supported by KOSEF NRL program (No. R0A-2008-000-20052-0). The computations were carried out at KISTI (KSC-2007-S00-1006).

<sup>1</sup>E. P. Gusev, V. Narayanan, and M. M. Frank, *IBM J. Res. Dev.* **50**, 387 (2006).

<sup>2</sup>S. C. Song, C. S. Park, J. Price, C. Burham, R. Choi, H. H. Tseng, B. H. Lee, and R. Jammy, *Tech. Dig. - Int. Electron Devices Meet.* **2007**, S13.3.

<sup>3</sup>H. Y. Yu, C. Ren, Y. C. Yeo, J. F. Kang, X. P. Wang, H. H. H. Ma, M. F. Li, D. S. H. Chan, and D. L. Kwong, *IEEE Electron Device Lett.* **25**, 337 (2004).

<sup>4</sup>J. Robertson, O. Sharia, and A. A. Demkov, *Appl. Phys. Lett.* **91**, 132912 (2007).

<sup>5</sup>S. Guha and V. Narayanan, *Phys. Rev. Lett.* **98**, 196101 (2007).

<sup>6</sup>J. K. Schaeffer, L. R. C. Fonseca, S. B. Samavedam, Y. Liang, P. J. Tobin, and B. E. White, *Appl. Phys. Lett.* **85**, 1826 (2004).

<sup>7</sup>Y. Akasaka, G. Nakamura, K. Shiraishi, N. Umezawa, K. Yamabe, O. Ogawa, M. Lee, T. Amiaka, T. Kasuya, H. Watanabe, T. Chikyow, F. Ootsuka, Y. Nara, and K. Nakamura, *Jpn. J. Appl. Phys., Part 2* **45**, L1289 (2006).

<sup>8</sup>H. Takeuchi, H. Y. Wong, D. Ha, and T.-J. King, *Tech. Dig. - Int. Electron Devices Meet.* **2004**, 829.

<sup>9</sup>D. Lim, R. Haight, M. Copel, and E. Cartier, *Appl. Phys. Lett.* **87**, 072902 (2005).

<sup>10</sup>A. V. Gavrikov, A. A. Knizhnik, A. A. Bagatur'yants, B. V. Potapkin, L. R. C. Fonseca, M. W. Stoker, and J. Schaeffer, *J. Appl. Phys.* **101**, 014310 (2007).

<sup>11</sup>G. Kresse and J. Hafner, *Phys. Rev. B* **47**, 558 (1993); **49**, 14251 (1994).

<sup>12</sup>P. E. Blöchl, *Phys. Rev. B* **50**, 17953 (1994).

<sup>13</sup>D. M. Ceperley and B. J. Alder, *Phys. Rev. Lett.* **45**, 566 (1980).

<sup>14</sup>A. S. Foster, F. Lopez Gejo, A. L. Shluger, and R. M. Nieminen, *Phys. Rev. B* **65**, 174117 (2002).

<sup>15</sup>D. M. Duffy, J. H. Harding, and A. M. Stoneham, *J. Appl. Phys.* **76**, 2791 (1994).

<sup>16</sup>C. Tang, B. Tuttle, and R. Ramprasad, *Phys. Rev. B* **76**, 073306 (2007).

<sup>17</sup>S. H. Jeon, B. Park, J. Lee, B. Lee, and S. Han, *Appl. Phys. Lett.* **89**, 042904 (2006).

<sup>18</sup>K. Shiraishi, Y. Akasaka, S. Miyazaki, T. Nakayama, T. Nakaoka, G. Nakamura, K. Torii, H. Furutou, A. Ohta, P. Ahmet, K. Ohmori, H. Watanabe, T. Chikyow, M. L. Green, Y. Nara, and K. Yamada, *Tech. Dig. - Int. Electron Devices Meet.* **2005**, 39.

<sup>19</sup>K. Xiong, P. W. Peacock, and J. Robertson, *Appl. Phys. Lett.* **86**, 012904 (2005).